Proceedings of International Design Engineering Technical Conferences & Computers and Information in Engineering Conference
IDETC-CIE
August 17, 2025, Anaheim, California

IDETC-169129

SURFACE ROUGHNESS SURROGATE MODELING IN METAL 3D PRINTING USING KRIGING AND BATCH EXPERIMENTAL DESIGN

Matthew Burnett
Department of
Mechanical Engineering
University of South Carolina
Columbia, South Carolina 29208
Email: matthew.burnett@sc.edu

Tianyu Zhang
Department of
Mechanical Engineering
University of South Carolina
Columbia, South Carolina 29208
Email: TZ5@email.sc.edu

Austin R.J. Downey
Department of
Mechanical Engineering
Department of Civil and
Environmental Engineering
University of South Carolina
Columbia, South Carolina 29208
Email: austindowney@sc.edu

Lang Yuan
Department of
Mechanical Engineering
University of South Carolina
Columbia, South Carolina 29208
Email: LANGYUAN@cec.sc.edu

ABSTRACT

Laser Powder Bed Fusion Additive Manufacturing has revolutionized the production of geometrically complex components, enabling the creation of intricate designs that were previously difficult or impossible to achieve using traditional manufacturing methods. However, one of the key challenges associated with laser powder bed fusion is the substantial surface roughness that often results in parts produced through this process. The increased surface roughness negatively impacts the mechanical performance of the components and increases the costs associated with post-processing, such as additional polishing or finishing treatments. This study seeks to address this challenge by developing a surrogate model for predicting and controlling vertical surface roughness based on process parameters. To achieve this, we propose the Kriging with Iterative Spatial Prediction (KRISP-Uncertainty) algorithm, which combines regression Kriging with an iterative leave-one-out cross-validation method that utilizes Kullback-Leibler Divergence (KLD). This approach refines the surrogate model using select experimental data points, reducing uncertainty with minimal additional experimental data. Our findings demonstrate that the KRISP-Uncertainty algorithm can effectively optimize surface roughness predictions, providing an efficient method for surrogate modeling and controlling surface quality in laser powder bed fusion. By rapidly tailoring stochastic surrogate models to specific material and hardware configurations, this method enhances the overall efficiency and effectiveness of the laser powder bed fusion process, reducing both surface roughness and the associated post-processing requirements.

1 Introduction

Laser powder bed fusion additive manufacturing is a common additive manufacturing technique used in aerospace or biomedical applications. Instead of machining metal away from feedstock, a laser is used to selectively fuse metal powder to-

Copyright © 2025 by ASME

gether layer by layer. Laser powder bed fusion enables the production of very geometrically complex components far beyond what can be achieved by traditional subtractive manufacturing methods. Laser powder bed fusion, however, often results in high surface roughness owing to the powder fusion process [1]. Controlling roughness is crucial; biomedical implants benefit from high roughness [2] for bonding, while mechanical systems require smooth surfaces to reduce friction and improve fatigue life [3]. While post-processing can reduce roughness, it adds cost and lead time.

Surface roughness is dependent on several process parameters (laser power, hatch distance, layer thickness, scan speed) and material properties [4]. While the overarching trends of how these parameters affect the surface roughness are reasonably well defined, exceptionally precise control of surface roughness will be very specific to the hardware and material used [5].

A high-fidelity surrogate model predicting vertical roughness must capture both general trends and stochastic behavior. This study proposes KRISP-Uncertainty, an algorithm that employs a regression Kriging surrogate model refined via leave-one-out cross-validation, identifying regions needing more data. The leave-one-out cross-validation model is scored with Kullback-Leibler Divergence [6]. KLD is an asymmetric divergence used to measure the relative entropy of two distributions ($P(x)$ $Q(x)$). KLD has become popular for uncertainty quantification approaches due to its ability to robustly quantify the divergence of spaces [7].

Pairing Kriging with an iterative cross-validation technique enables minimal testing while effectively characterizing the design space for real-world use [8]. Cao et al., for example, used Kriging in conjunction with a whale optimization algorithm to characterize the surface roughness of as-built components with respect to their process parameters [9]. In that study, a Kriging metamodel is built, experimentally validated, and then searched with whale optimization. The Kriging-based uncertainty quantification approach proposed in this paper looks to specifically improve the construction of the Kriging metamodels.

This work proposes and validates KRISP-Uncertainty, an experimental design algorithm used to predict uncertainty spatially in stochastic domains. The contributions of this study are twofold: 1) developing a novel iterative experimental design algorithm combining regression Kriging and leave-one-out cross-validation with KLD to minimize model uncertainty; and 2) experimentally validating this methodology through targeted measurements of vertical surface roughness in laser powder bed fusion additive manufacturing, demonstrating significant improvements in predictive accuracy and efficiency.

2 Methodology

The proposed algorithm diagrammed in figure 1, combines the predictive power of Kriging with a statistical uncertainty

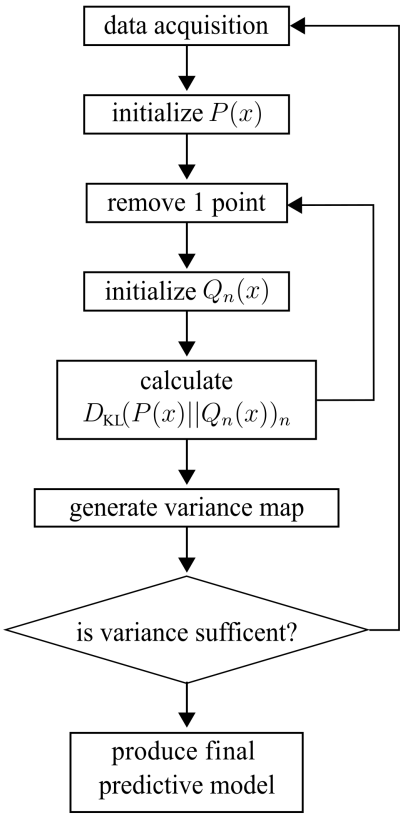

FIGURE 1. A flow chart outlining the design of experiment algorithm process.

analysis model to quantify uncertainty spatially. A "ground truth" ($P(x)$) is generated by training a Kriging model with the entire training set. This ground truth is then compared to models each with one data point removed ($Q_n(x)$). For each iteration there will be one $P(x)$ and n, $Q_n(x)$ distributions. In this section $P(x)$ and $Q_n(x)$ are arbitrary distributions but for this application specifically $P(x)$ would be the surface roughness with respect to the process parameters or, $S_{\mathrm{a}}(\mathrm{power}, \mathrm{speed})$

Once the KLD scores, $D_{\mathrm{KL}}(P(x) \parallel Q_n(x))$, are calculated, they are then assigned to the point missing in that respective model. It can be assumed that if the removal of a point induces considerable error in the area surrounding that point, the region is uncertain. The spatial map of the KLD scores is then generated by interpolating the error with respect to each point. It should be noted that though this study chose Kriging paired with KLD for reasons discussed below, any predictive model and loss function can be used with this technique. The KLD from continuous distribution P to continuous distribution Q is defined as

Copyright © 2025 by ASME

$$D_{\mathrm{KL}}(P \parallel Q) = \int P(x) \log \frac{P(x)}{Q(x)}\, dx. \tag{1}$$

To summarize the algorithm described in figure 1 the abbreviated list of steps is shown below.

1. **Ground truth** $P(x)$: train Kriging on full dataset.
2. **Leave-one-out** $Q_i(x)$: retrain without point i.
3. **Uncertainty metric**: compute KLD with equation 1 and assign each score to the omitted location.
4. **Spatial map**: interpolate the KLD scores across the domain to highlight regions of high uncertainty.

2.1 Kriging

Universal Kriging treats spatial data as a Gaussian process, providing both interpolated values and confidence intervals. It models observations as

$$Z(x) = \mu(x) + \delta(x), \tag{2}$$

where $\mu(x)$ is a drift term (fit by regression) and $\delta(x)$ is the local variation. The Universal Kriging (UK) estimate at x_0 is

$$\hat{z}(x_0) = \hat{m}(x_0) + \hat{e}(x_0), \tag{3}$$

with trend

$$\hat{m}(x_0) = q_0^{\mathrm{T}} \hat{\beta} \tag{4}$$

and residuals weighted by the kriging weights λ_0:

$$\hat{e}(x_0) = \lambda_0^{\mathrm{T}} e, \tag{5}$$

so that

$$\hat{z}(x_0) = q_0^{\mathrm{T}} \hat{\beta} + \lambda_0^{\mathrm{T}} e. \tag{6}$$

Here, q_0 is the vector of basis functions at x_0, $\hat{\beta}$ are the estimated drift coefficients, e is the vector of residuals at the sampled points, and λ_0 are the kriging weights.

The variance at x_0 is

$$\sigma^2(x_0) = n - c_0^{\mathrm{T}} C^{-1} c_0 + (q_0 - q^{\mathrm{T}} C^{-1} c_0)^{\mathrm{T}} (q^{\mathrm{T}} C^{-1} q)^{-1} (q_0 - q^{\mathrm{T}} C^{-1} c_0). \tag{7}$$

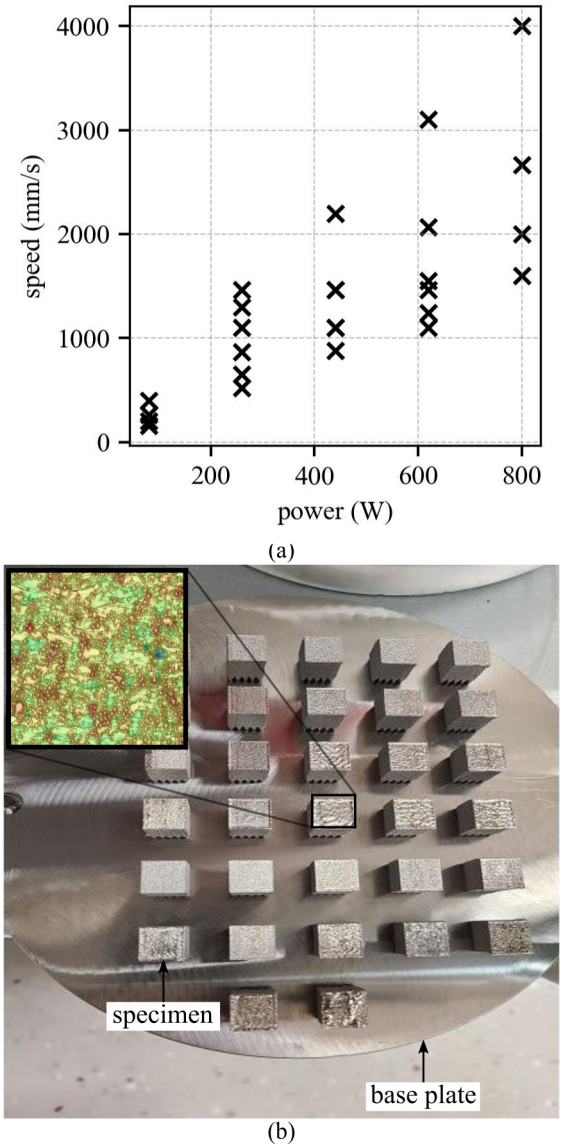

FIGURE 2. Example test set in the sample space, showing: (a) outline of all initially tested points; (b) a test bed from the printer and a depth map example from Dataset 1.

Universal Kriging effectively integrates spatial variability and regression trends to generate accurate predictive models and quantify uncertainty. This study extends the universal Kriging approach by using regression Kriging, where a regression model captures broad trends and universal Kriging accounts for the spatially correlated residuals. By leveraging regression Kriging, the predictive accuracy and efficiency of the spatial model are enhanced, making it especially effective for iterative refinement and uncertainty quantification.

Copyright © 2025 by ASME

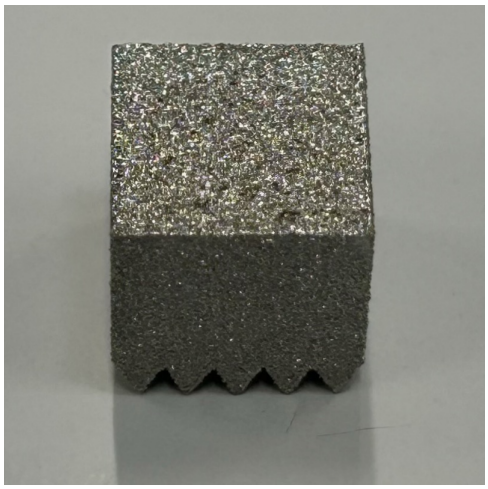

FIGURE 3. Example of a cube used for surface roughness tests.

2.2 Experimental Data Collection

The laser power and speed were varied across different test locations seen in figure 2 to build a dataset to predict the vertical surface roughness of as-built components. The material selected for this study was 316L stainless steel. For all experiments, cubes were printed with a hatch distance of 100 µm and a layer thickness of 30 µm.

By obtaining a depth map, the surface roughness (S_a) value could be derived as

$$S_a = \frac{1}{A}\int_A |z(x,y)|\,dx\,dy, \tag{8}$$

where A is the evaluation area, and $z(x,y)$ is the height of the surface at a point (x,y) relative to the mean plane. S_a was obtained for both top and vertical surface roughness for all components, however, this study focuses on the modeling of vertical surface roughness. Figure 3 shows an example of a cube used for surface roughness tests.

Over the course of this study, an initial dataset of 26 experimental points was built on iteratively. When new data was collected it was appended to the initial dataset. In total three datasets were generated each with a few more points than the last. The number of points in each set is outlined in table 1. Upon collecting an initial 26 data points, a series of numerical experiments were done to decide upon the interpolation model for the algorithm. Previous literature has already shown the applicability of using Kriging for the optimization of surface roughness [9].

In this study, three models were tested with the leave-one-out cross-validation scheme to assess their fitting and predictive capacity. Leave-one-out cross-validation iteratively removes one point from the dataset, trains on the rest, and then produces a prediction of each of the missing points. Linear regression, Universal Kriging, and Regression Kriging with linear regression and ordinary Kriging were tested. Table 2 outlines the performance of each model when trained on the initial dataset.

TABLE 1. A description of each dataset listed in this study.

dataset	number of points
Dataset 1	26
Dataset 2	33
Dataset 3	41

TABLE 2. Performance metrics for each model.

	RK	UK	OK	linear regression
MSE	23.00	86.37	86.37	26.27
MAE	3.46	7.19	7.19	3.84
MAPE	17%	32%	32%	18%

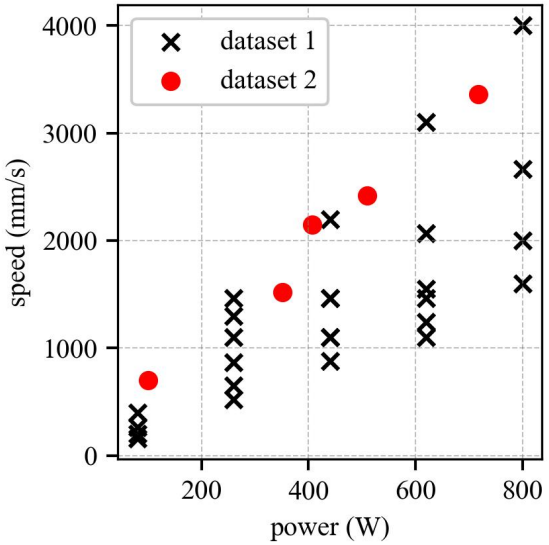

FIGURE 4. An outline of all initially tested points in the sample space in addition to the newly added sample locations from test 2 .

Due to the superior performance of RK, it was selected as the model for the remainder of the study. The first set of experimental data was interpolated using regression Kriging and the variance was assessed with the algorithm described above in figure 1. The initial regression Krige and sensitivity analysis is shown in figure 5.

Following the sensitivity analysis, a series of additional samples were acquired to improve model performance which can be seen in figure 4. The additional samples were selected from the

Copyright © 2025 by ASME

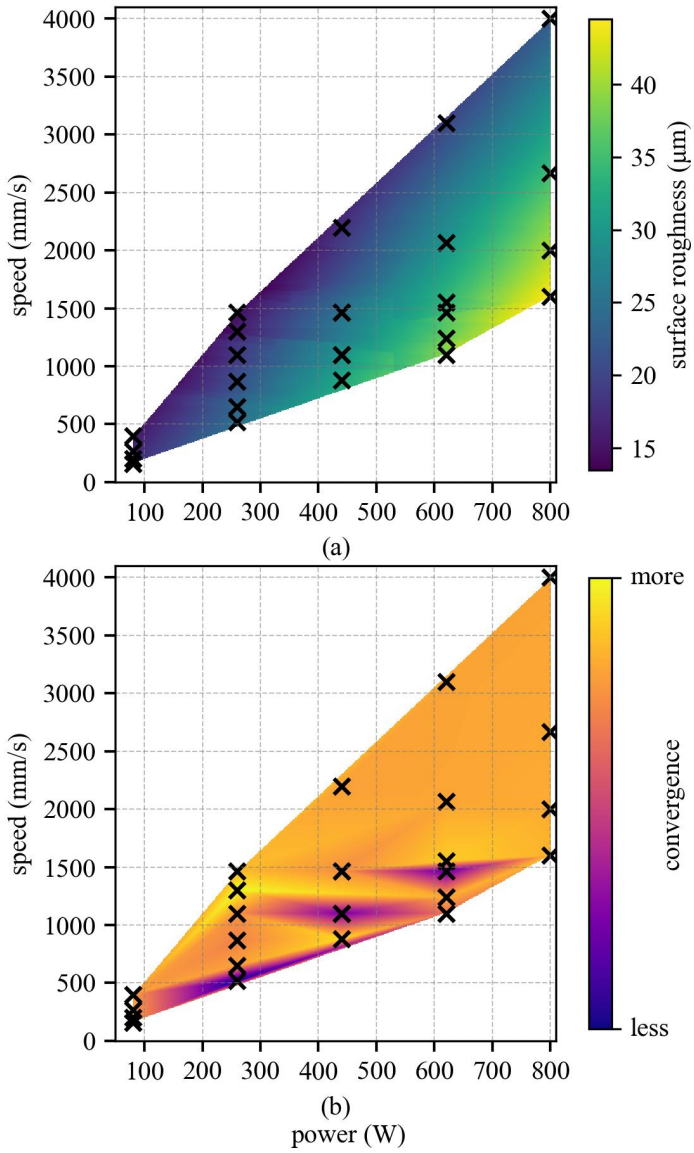

FIGURE 5. RK predictions of surface roughness and spatial sensitivity analysis for Dataset 1, showing: (a) surface roughness; and (b) spatial sensitivity for Dataset 1.

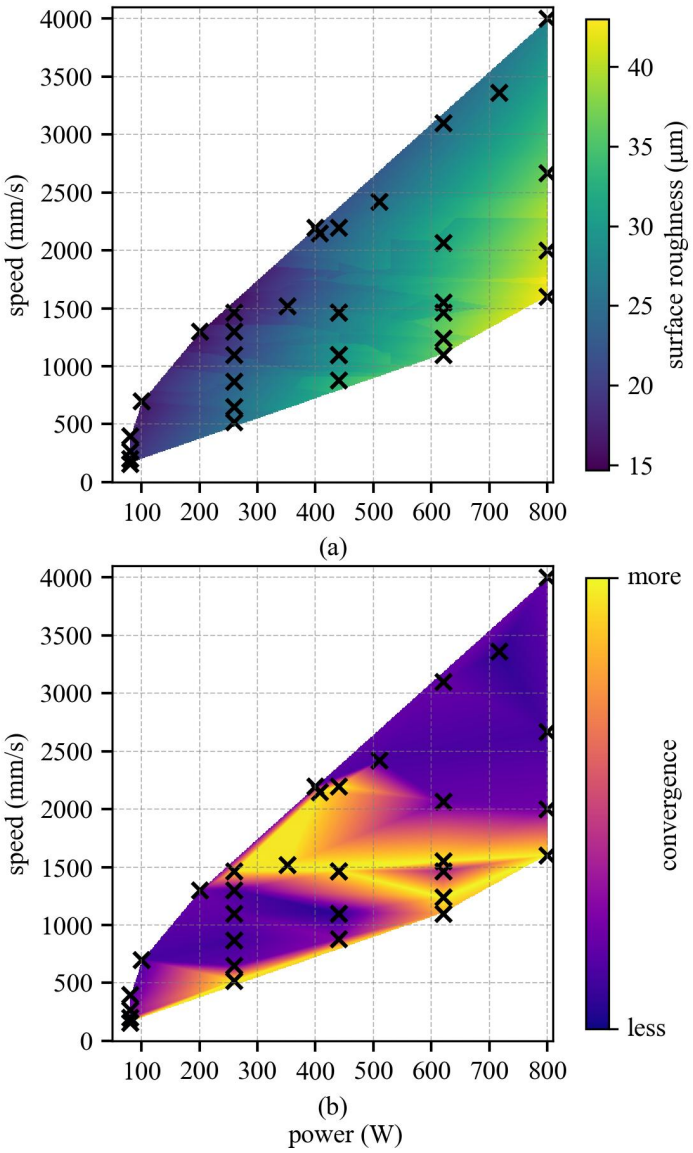

FIGURE 6. RK predictions of surface roughness and spatial sensitivity analysis for Dataset 2, showing: (a) surface roughness; and (b) spatial sensitivity for Dataset 2.

high-sensitivity regions marked by the initial sensitivity analysis. It can be seen in figure 6 that the sensitivity dropped considerably across most of the domain, particularly in the high power and speed and low power and speed regions.

3 Results and Discussion

To enhance the predictive accuracy and reliability of the vertical surface roughness model, an additional round of data collection was performed. Each iteration of data acquisition was informed by a spatial sensitivity analysis, which identified regions with high model uncertainty and guided sample placement for optimal refinement. To enhance the predictive accuracy and reliability of the vertical surface roughness model, an additional round of data collection was performed. Each iteration of data acquisition was informed by a spatial sensitivity analysis, which identified regions with high model uncertainty and guided sample placement for optimal refinement. The first dataset com-

Copyright © 2025 by ASME

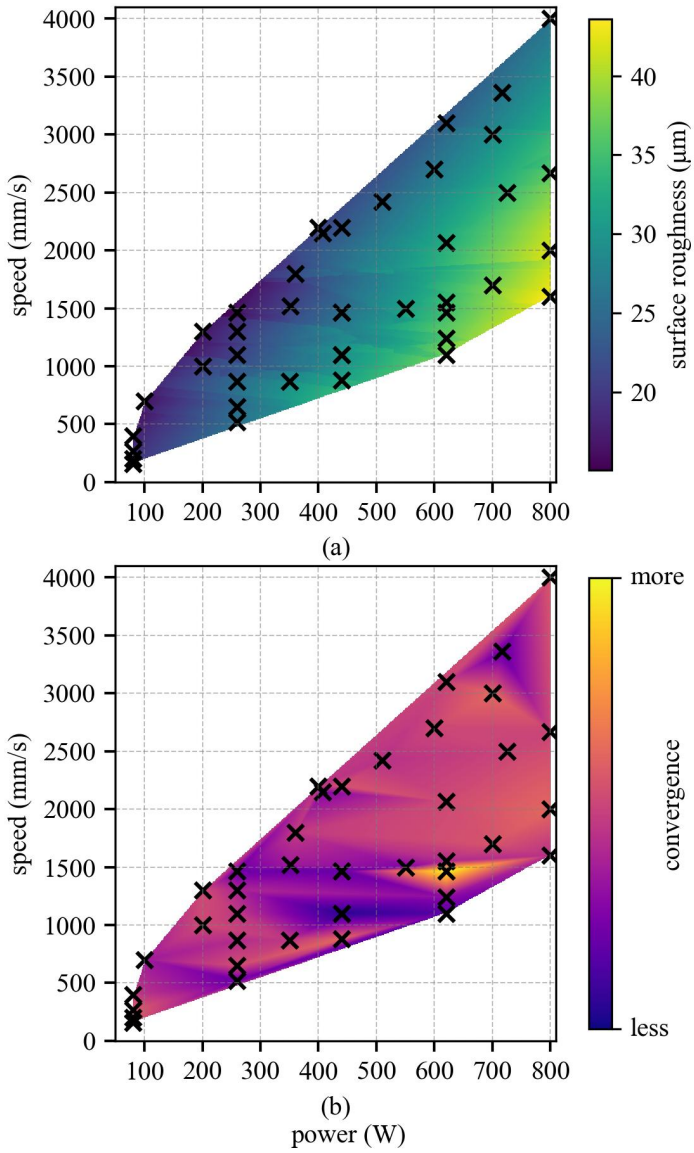

FIGURE 7. RK predictions of surface roughness and spatial sensitivity analysis for Dataset 3, showing: (a) surface roughness; and (b) spatial sensitivity for Dataset 3.

prised 26 sample locations, strategically chosen based on initial process parameter variations. After assessing the model's predictive performance and identifying high-sensitivity regions, a second dataset with 33 samples was obtained by adding the initial data with the newly collected data, focusing on areas where the model exhibited significant uncertainty. Finally, a third dataset expanded the sampling coverage to 41 locations, further improving model convergence. This iterative approach ensured that additional data points were placed in areas where they would have

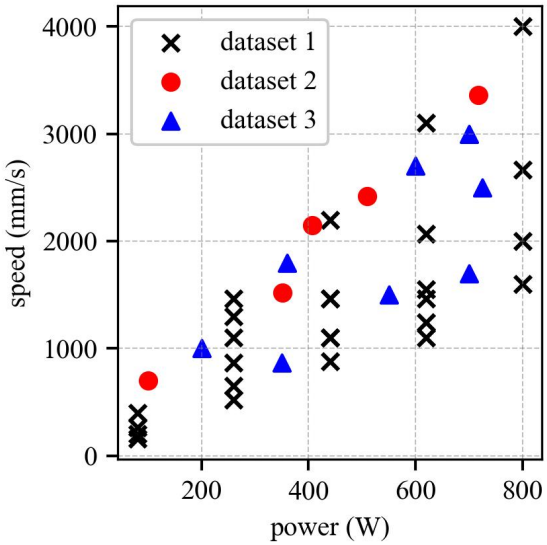

FIGURE 8. An outline of all initially tested points in the sample space in addition to the newly added sample locations from tests 2 and 3.

TABLE 3. Performance metrics of Dataset 1 and Dataset 2 with respect to the final dataset.

	MSE	MAE	MAPE	number of samples
Dataset 1	1.52	1.01	2.35%	26
Dataset 2	0.68	0.69	1.72%	33

the highest impact on reducing prediction errors, leading to a more robust and generalizable surface roughness model. The final dataset, seen in figure 7, demonstrated a marked improvement in predictive accuracy, as reflected in reduced mean squared error (MSE), mean absolute error (MAE), and mean absolute percentage error (MAPE) when compared to earlier models.

A ground truth was established for the sample space to effectively compare the improvement between Dataset 1 and Dataset 2. A third and final series of tests were performed to act as ground truth and allow for a retrospective comparison of the original and refined model. Figure 8 outlines the added sample locations.

The final converged model allows for a direct comparison between the initial and refined models. MSE, MAE, and MAPE were calculated for datasets 1 and 2 relative to Dataset 3, which serves as the 'ground truth.' The entire sample space predictions were evaluated against Dataset 3, and Table 3 summarizes the errors for datasets 1 and 2.

To quantify the performance improvements, the error metrics for Dataset 1 and Dataset 2 were evaluated relative to Dataset 3. Table 3 presents the results, illustrating a clear reduc-

Copyright © 2025 by ASME

tion in errors as additional data was incorporated. The second dataset showed significant improvement over the first, with MSE decreasing from 1.52 to 0.68 and MAPE dropping from 2.35% to 1.72%. The reduction in maximum error further demonstrates how the iterative refinement process led to a more reliable and generalizable model.

4 Conclusion

This study has demonstrated the effectiveness of the KRISP-Uncertainty algorithm in making and refining predictions of vertical surface roughness in laser powder bed fusion. Through successive rounds of data collection and spatial sensitivity analysis, the model successfully identified high-uncertainty regions, allowing for targeted sample placement and improved predictive accuracy. The results confirmed the model's ability to optimize surface roughness predictions while minimizing sampling. With the addition of only 7 points the model's average error was reduced by 68.3%.

The findings also reinforce the well-established influence of process parameters, particularly laser power, on surface roughness. This study further highlights the importance of an adaptive data-driven approach in refining predictive models. The use of Kullback-Leibler Divergence (KLD) in the design of the experiments framework provided a systematic Bayesian method for improving model accuracy, ensuring that additional data collection was focused on areas of greatest uncertainty.

Future work could explore integrating additional factors such as scan strategy and powder properties to further enhance model robustness. Additionally, applying this methodology to real-time monitoring and control in laser powder bed fusion could provide a path toward adaptive manufacturing processes. Overall, the results demonstrate a practical and efficient approach to improving surface roughness modeling, contributing to enhanced process optimization and quality control in additive manufacturing.

ACKNOWLEDGMENTS

This material is based upon work supported (algorithms) by the National Science Foundation grant numbers ITE - 2344357, and CMMI - 2152896; In addition to work from the Office of Naval Research through award number 14048906 Moreover, support for 3D printing aspects of this work was partially supported by the U.S. Department of Commerce, National Institute of Standards and Technology through award number 70NANB23H030 Any opinions, findings conclusions, or recommendations expressed in this material are those of the authors and do not necessarily reflect the views of the National Science Foundation, the U.S. Department of Commerce, or the United States Navy.

REFERENCES

[1] Snyder, J. C., and Thole, K. A., 2020. "Understanding laser powder bed fusion surface roughness". *Journal of Manufacturing Science and Engineering,* ***142***(7), 05, p. 071003.

[2] Lewallen, E. A., Riester, S. M., Bonin, C. A., Kremers, H. M., Dudakovic, A., Kakar, S., Cohen, R. C., Westendorf, J. J., Lewallen, D. G., and van Wijnen, A. J., 2015. "Biological strategies for improved osseointegration and osteoinduction of porous metal orthopedic implants". *Tissue Engineering. Part B, Reviews,* ***21***(2), pp. 218–230.

[3] Nakatani, M., Masuo, H., Tanaka, Y., and Murakami, Y., 2019. "Effect of surface roughness on fatigue strength of ti-6al-4v alloy manufactured by additive manufacturing". *Procedia Structural Integrity,* ***19***, pp. 294–301. Fatigue Design 2019, International Conference on Fatigue Design, 8th Edition.

[4] Dejene, N. D., Lemu, H. G., and Gutema, E. M., 2024. "Effects of process parameters on the surface characteristics of laser powder bed fusion printed parts: machine learning predictions with random forest and support vector regression". *The International Journal of Advanced Manufacturing Technology,* ***133***(11), pp. 5611–5625.

[5] Zhang, T., and Yuan, L., 2024. "Interaction of contour and hatch parameters on vertical surface roughness in laser powder bed fusion". *Journal of Materials Research and Technology,* ***32***, pp. 3390–3401.

[6] Kullback, S., and Leibler, R. A., 1951. "On information and sufficiency". *The Annals of Mathematical Statistics,* ***22***(1), pp. 79–86.

[7] Downey, A., Sadoughi, M., Laflamme, S., and Hu, C., 2018. "Incipient damage detection for large area structures monitored with a network of soft elastomeric capacitors using relative entropy". *IEEE Sensors Journal,* ***18***(21), pp. 8827–8834.

[8] Andrea Meoni, Enrique García-Macías, I. V., and Ubertini, F., 2023. "A procedure for bridge visual inspections prioritisation in the context of preliminary risk assessment with limited information". *Structure and Infrastructure Engineering,* ***21***(3), pp. 394–420.

[9] Cao, L., Li, J., Hu, J., Liu, H., Wu, Y., and Zhou, Q., 2021. "Optimization of surface roughness and dimensional accuracy in lpbf additive manufacturing". *Optics and Laser Technology,* ***142***, p. 107246.

Copyright © 2025 by ASME